Resonancelike enhancement in high-order above-threshold ionization of polyatomic molecules

C. Wang,[1] M. Okunishi,[2] X. Hao,[3,*] Y. Ito,[2] J. Chen,[4,5,†] Y. Yang,[1] R. R. Lucchese,[6] M. Zhang,[1]
B. Yan,[1] W. D. Li,[3] D. Ding,[1,‡] and K. Ueda[2,§]

[1]*Institute of Atomic and Molecular Physics, Jilin University, Changchun 130012, PR China*

[2]*Institute of Multidisciplinary Research for Advanced Materials, Tohoku University, Sendai 980-8577, Japan*

[3]*Institute of Theoretical Physics and Department of Physics, Shanxi University, 030006 Taiyuan, China*

[4]*CAPT, HEDPS, and IFSA Collaborative Innovation Center of MoE College of Engineering, Peking University, Beijing 100084, China*

[5]*Institute of Applied Physics and Computational Mathematics, P. O. Box 8009, Beijing 100088, China*

[6]*Department of Chemistry, Texas A&M University, College Station, Texas 77843-3255, USA*

We investigate the resonance-like enhancement (RLE) in high-order above-threshold ionization (ATI) spectra of the polyatomic molecules C_2H_4 and C_2H_6. In the spectrum-intensity maps, strong and weak RLE areas emerge alternatively for both C_2H_4 and C_2H_6 but in different sequences. Theoretical calculations using the strong-field approximation reproduce the experimental observation and analysis shows that the different characteristics of the two molecules can be attributed to interference effects of molecular orbitals with different symmetries. For C_2H_4, the RLE structures are attributed to C–C centers of the highest occupied molecular orbital (HOMO) orbital. For C_2H_6, in contrast, the C–C centers of the HOMO and HOMO-1 orbitals do not contribute to the RLE due to destructive interference but the hydrogen centers of the bonding HOMO-1 orbital give rise to the multiple RLE regions. In addition, clear experimental evidence of the existence of two types of the RLE and their dependence on the parity of ground state is shown. Our result, which strongly supports the channel-closing mechanism of the RLE, for the first time reveals the important role of low-lying orbitals and the differing roles of different atomic centers in the high-order ATI spectrum of molecules.

Imaging ultrafast atomic and molecular dynamics and structures has been made possible by advances in the understanding of the interactions between atoms and molecules and ultrashort intense laser pulses [1,2]. Novel methods such as laser-induced electron diffraction (LIED) [3] and orbital tomography [4–7] have been developed to image molecular structures on an attosecond timescale and an angstrom spatial scale. All these methods are built on the recollision mechanism [8,9], which constitutes the foundation of our understanding of atomic and molecular dynamics in intense laser fields. For the high-energy part of the molecular above-threshold ionization (ATI) spectrum, the structure of the highest occupied molecular orbital (HOMO) has been found to play important role [10–12]. However, the low-lying molecular orbitals, whose importance have been demonstrated in molecular high-harmonic-generation processes [6,7,13], still elude observation in the high-order ATI (HATI) spectrum. On the other hand, although it has been widely accepted that the recollision picture can explain the overall structure of the HATI spectrum, an intriguing effect called "resonancelike enhancement" (RLE) observed in the plateau regime of the spectrum has been the source of much debate concerning its underlying mechanism but no consensus has been achieved so far [14–21]. Groups of HATI peaks (higher than $2U_p$) show unusual intensity-dependent enhancement which was at first identified for noble gas atoms: when the laser peak intensity changes only slightly, the magnitudes of HATI peaks, located at $6U_p$ and $8U_p$, can exhibit significant enhancement by up to an order of magnitude [14,15]. Two mechanisms have been proposed to explain the RLE. In the framework of the "quantum orbits" theory, the RLE is attributed to constructive interference of a large number of electronic trajectories with small momenta when the electrons return to the ionic core which happens near channel closings [20–22]. It is assumed that the ionization potential of the molecule is raised in energy with the amount of U_p; as U_p increases, the absorption of n photons (photon energy is 1.55 eV in our case) no longer suffices for ionization and $n + 1$ photons are required; in other words, the n-photon channel is closed, the so-called channel closing. In the Freeman resonance picture, the RLE structures originate from multiphoton resonance with intensity-dependent excited bound states [17–19]. Recently, the RLE structures were also experimentally observed for molecules [23,24]. Analysis indicates that the mechanism favors the channel-closing perspective [24].

We report on the experimental observation of the RLE structure for the two hydrocarbons C_2H_4 and C_2H_6 by measuring the HATI photoelectron spectrum. Both C_2H_4 and C_2H_6 show more than one intensity-dependent RLE modulations. The magnitudes of different RLE modulations differ greatly and the weak and strong RLE modulations emerge alternately with different sequences in the two molecules. These results can be well reproduced and understood by our theoretical calculations.

In our experiment, we used a linear time-of-flight (TOF) (264 mm) spectrometer with a small detection solid angle ($\sim 0.0014 \times 4\pi$ sr) to detect electrons. Intense 800 nm, 100 fs laser pulses (repetition rate of 1 kHz) from an amplified

*xlhao@sxu.edu.cn

†chen_jing@iapcm.ac.cn

‡dajund@jlu.edu.cn

§ueda@tagen.tohoku.ac.jp
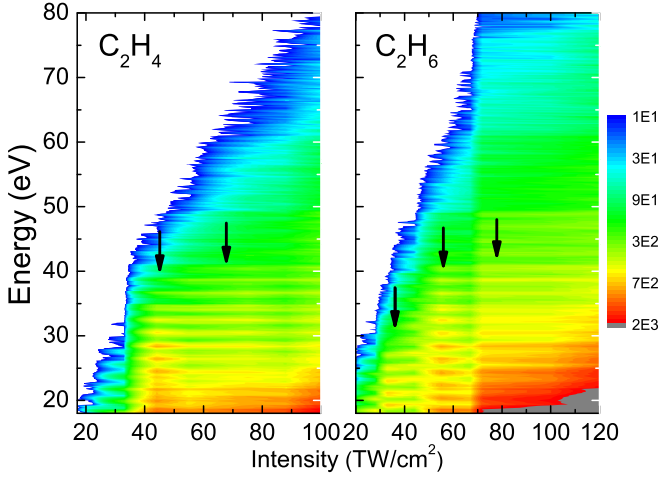
FIG. 1. The measured ATI spectra of C_2H_4 and C_2H_6 covering a wide intensity range. The horizontal axis reflects the laser intensity and the vertical axis gives the kinetic energy of ATI electrons. The false-color scale reflects the ionization yields. The bright yellow horizontal lines indicate the RLE structures (marked by arrows), as discussed in the text.

FIG. 2. The experimental electron kinetic energy spectra of C_2H_4 [panels (a) and (b)] and C_2H_6 [panels (c) and (d)]. Only the plateau regions are shown for comparison of different types of RLE. The numbers given in the legends are peak laser intensities with units of TW/cm^2.

Ti:sapphire laser system were used to ionize the molecules. The laser beam was focused by an $f = 100$ mm mirror to an effusively introduced C_2H_4 and C_2H_6 gas in a vacuum chamber. To estimate the peak intensity of the laser pulse, we used the well-known $10U_p$ cutoff in the HATI spectra of Xe [25]. Further details of the experimental setup and procedure are given elsewhere [26,27].

Figure 1 depicts the measured ATI spectra of C_2H_4 and C_2H_6 evolving as functions of the laser intensity. To construct the two-dimensional image of Fig. 1, the ATI spectrum was normalized at each laser intensity to clearly emphasize the overall evolution of the spectra with the laser intensity. The energy range ($10U_p$ cutoff) extended nearly linearly with increasing laser intensity for both molecules, indicating that the laser intensity is well below saturation. Directly ionized electrons (lower than $2U_p$) are omitted here and only high-energy electrons in the plateau region are shown. Both C_2H_4 and C_2H_6 show multiple RLE features in different energy regions with increasing laser intensity. For C_2H_4, the bright yellow horizontal lines between 20–30 eV indicate that the RLE appears around 40 TW/cm^2. As can be clearly seen in Fig. 2(a), nearly a one-order-of-magnitude enhancement is observed at 44 TW/cm^2 and then the ATI peaks are suppressed at higher intensity, e.g., 55 TW/cm^2. As the laser intensity increases, another weaker RLE modulation appears around 70 TW/cm^2, as can also be seen in Fig. 2(b). For C_2H_6, at least three RLE modulations can be seen in Fig. 1(b). Similar to C_2H_4, the weak and strong RLEs appear alternately. The first RLE at 33 TW/cm^2 is weak whereas the second one at 55 TW/cm^2 is very strong [see Figs. 2(c) and 2(d)].

Why do two polyatomic molecules show different types of RLE structure? As mentioned before, the mechanism responsible for the RLE is still uncertain. For atoms, both numerical solutions of the time-dependent Schrödinger equation [17–19] and strong-field approximation (SFA) [20–22] can reproduce the experimental observation. Thus far for
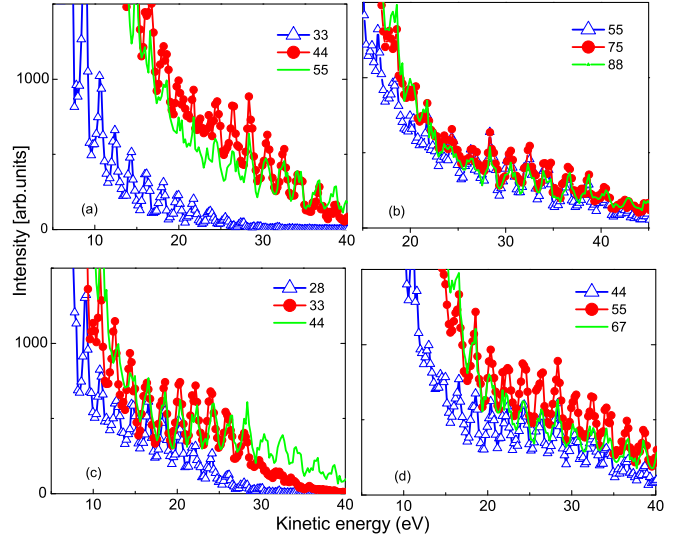
molecules, only the SFA has been adopted and succeeded in explaining the appearance and absence of the RLE in N_2 and O_2 molecules [24]. To explore the underlying physics, we employ here the SFA theory [28] to simulate the ATI spectrum.

The transition amplitude is (atomic units $m = \hbar = e = 1$ are used)

$$M_{\mathbf{p}} = M_{\mathbf{p}}^{\text{dir}} + M_{\mathbf{p}}^{\text{resc}}, \qquad (1)$$

where

$$M_{\mathbf{p}}^{\text{dir}} = -i \int_{-\infty}^{\infty} dt' \langle \psi_{\mathbf{p}}^{(V)}(t') | \mathbf{r} \cdot \mathbf{E}(t') | \psi_0(t') \rangle \qquad (2)$$

is the amplitude for the direct electrons, and

$$M_{\mathbf{p}}^{\text{resc}} = -\int_{-\infty}^{\infty} dt \int_{-\infty}^{t} dt' \int d^3\mathbf{k} \langle \psi_{\mathbf{p}}^{(V)}(t) | V | \psi_{\mathbf{k}}^{(V)}(t) \rangle$$
$$\times \langle \psi_{\mathbf{k}}^{(V)}(t') | \mathbf{r} \cdot \mathbf{E}(t') | \psi_0(t') \rangle \qquad (3)$$

describes the rescattering process. Here $|\psi_0(t)\rangle$ is the ground state, $|\psi_{\mathbf{p}}^{(V)}(t)\rangle$ is the Volkov state with asymptotic momentum $\mathbf{p}$, and V denotes the binding potential.

The molecular initial state $|\psi_0(t)\rangle$, within the fixed-nuclei approximation, can be written as a linear combination of atomic orbitals (LCAO). Although the polyatomic molecules we consider here look very complex, they both have inversion symmetry, so that the orbitals can be characterized as either g or u symmetry. The C_2H_4 molecule has D_{2h} symmetry and the C_2H_6 molecule has D_{3d} symmetry. The resulting LCAO orbitals can be written as combinations of atomic-orbital pairs. In each pair, the two centers of the atomic orbitals are symmetric about the origin just as in a homonuclear diatomic molecule so that pairs of atomic orbitals form symmetric and antisymmetric combinations:

$$\psi_0(\mathbf{r}) = \sum_a c_a \big[\psi_a^{(0)}(\mathbf{r} + \mathbf{R}_a/2) + \gamma \psi_a^{(0)}(\mathbf{r} - \mathbf{R}_a/2) \big], \quad (4)$$

TABLE I. The composition of the molecular orbitals.

	C_2H_4	C_2H_6
HOMO$_1$	$(Cp\pi + Cp\pi)$	$(Cp\pi - Cp\pi)$
		$+(H+H)_1+(H+H)_2-2(H+H)_3$
HOMO$_2$		$(Cp\pi - Cp\pi)$
		$+(H+H)_1$-$(H+H)_2$
HOMO-1	$(Cp\sigma - Cp\sigma)$	$(Cp\sigma - Cp\sigma) - (H+H)_1$
	$-(H-H)_1 + (H-H)_2$	$-(H+H)_2 - (H+H)_3$

where $\mathbf{R}_a$ denotes the relative nuclear coordinate, the subscript a denotes different atom pairs and γ can be 1 or -1 depending on the symmetry. We show the contributions from the different centers of the molecules to the molecular orbitals in Table I. It is noted that there are two degenerate HOMOs for C_2H_6, which are distinguished by the subscript. The binding potential in Eq. (3) has the corresponding form

$$V(\mathbf{r}) = \sum_a V_a(\mathbf{r} + \mathbf{R}_a/2) + V_a(\mathbf{r} - \mathbf{R}_a/2), \quad (5)$$

where V_a denotes the atomic binding potential of the corresponding atom pair.

After substituting the wave function (4) into Eqs. (2) and (3) and employing the dressed modified molecular SFA [28], the transition amplitudes can be rewritten as

$$M_{\mathbf{p}}^{\text{dir}} = -i \int_{-\infty}^{\infty} dt' \sum_a c_a f_{\gamma,a}(\mathbf{p}, \mathbf{R}_a)$$
$$\times \langle \psi_{\mathbf{p}}^{(V)}(t') | \mathbf{r} \cdot \mathbf{E}(t') | \psi_a^{(0)}(t') \rangle \quad (6)$$

and

$$M_{\mathbf{p}}^{\text{resc}} = -\int_{-\infty}^{\infty} dt \int_{-\infty}^{t} dt' \int d^3\mathbf{k}$$
$$\times \sum_a 2 \cos[(\mathbf{p} - \mathbf{k}) \cdot \mathbf{R}_a/2] \langle \psi_{\mathbf{p}}^{(V)}(t) | V_a | \psi_{\mathbf{k}}^{(V)}(t) \rangle$$
$$\times \sum_{a'} c_{a'} f_{\gamma,a'}(\mathbf{k}, \mathbf{R}_{a'}) \langle \psi_{\mathbf{k}}^{(V)}(t') | \mathbf{r} \cdot \mathbf{E}(t') | \psi_{a'}^{(0)}(t') \rangle, \quad (7)$$

where

$$f_{\gamma,a}(\mathbf{k}, \mathbf{R}_a) = \begin{cases} 2\cos(\mathbf{k} \cdot \mathbf{R}_a/2), & \gamma = 1 \\ 2i\sin(\mathbf{k} \cdot \mathbf{R}_a/2), & \gamma = -1 \end{cases} \quad (8)$$

is the interference term between two atomic centers in one atom pair.

We use the saddle-point method to calculate the integrals in Eqs. (6) and (7), and the amplitudes can be written as

$$M_{\mathbf{p}}^{\text{dir}} = -i \int_{-\infty}^{\infty} dt' \exp[i S_{\mathbf{p}}(t')] V_{\mathbf{p}0} \quad (9)$$

and

$$M_{\mathbf{p}}^{\text{resc}} = -\int_{-\infty}^{\infty} dt \int_{-\infty}^{t} dt' \int d^3\mathbf{k} \exp[i S_{\mathbf{p}}(t,t',\mathbf{k})] V_{\mathbf{pk}} V_{\mathbf{k0}}, \quad (10)$$

with the actions given by

$$S_{\mathbf{p}}(t') = -\frac{1}{2} \int_{t'}^{\infty} d\tau [\mathbf{p} + \mathbf{A}(\tau)]^2 + I_p t' \quad (11)$$

and

$$S_{\mathbf{p}}(t,t',\mathbf{k}) = -\frac{1}{2} \int_{t}^{\infty} d\tau [\mathbf{p} + \mathbf{A}(\tau)]^2$$
$$- \frac{1}{2} \int_{t'}^{t} d\tau [\mathbf{k} + \mathbf{A}(\tau)]^2 + I_p t', \quad (12)$$

where I_p is the ionization potential of the orbital and $\mathbf{A}(t)$ is the vector potential. The prefactors in Eqs. (9) and (10) are

$$V_{\mathbf{k0}} = \frac{1}{(2\pi)^{3/2}} \sum_a c_a f_{\gamma,a}(\mathbf{k}, \mathbf{R}_a)$$
$$\times \int d^3\mathbf{r} \exp\{-i[\mathbf{k} + \mathbf{A}(t')] \cdot \mathbf{r}\} V(\mathbf{r}) \psi_a^{(0)}(\mathbf{r}) \quad (13)$$

and

$$V_{\mathbf{pk}} = \frac{1}{(2\pi)^3} \sum_a 2 \cos[(\mathbf{p} - \mathbf{k}) \cdot \mathbf{R}_a/2]$$
$$\times \int d^3\mathbf{r} \exp[-i(\mathbf{p} - \mathbf{k}) \cdot \mathbf{r}] V_a(\mathbf{r}). \quad (14)$$

For the rescattering amplitude (10), the saddle-point equations are

$$[\mathbf{k} + \mathbf{A}(t')]^2 = -2I_p, \quad (15)$$

$$[\mathbf{p} + \mathbf{A}(t)]^2 = [\mathbf{k} + \mathbf{A}(t)]^2, \quad (16)$$

$$\int_{t'}^{t} d\tau [\mathbf{k} + \mathbf{A}(\tau)] = 0. \quad (17)$$

Then the amplitudes can be approximated by

$$M_{\mathbf{p}}^{\text{dir}} = \sum_s \sqrt{\frac{2\pi i}{\partial^2 S_{\mathbf{p}}/\partial t_s'^2}} V_{\mathbf{p}0} \exp[i S_{\mathbf{p}}(t_s')] \quad (18)$$

and

$$M_{\mathbf{p}}^{\text{resc}} = \sum_s (2\pi i)^{5/2} \frac{V_{\mathbf{pk}_s} V_{\mathbf{k}_s,0}}{\sqrt{\det S_{\mathbf{p}}''(t,t',\mathbf{k})|_s}}$$
$$\times \exp[i S_{\mathbf{p}}(t_s, t_s', \mathbf{k}_s)], \quad (19)$$

where the index s runs over the relevant saddle points.

For some molecules, not only the HOMOs but also the lower-lying orbitals can substantially contribute to the ionization process. So in our calculations, both the HOMO and HOMO-1 orbitals are included. In Table II, we show the ionization potentials of different orbitals. The difference of ionization potential between HOMO and HOMO-1 for C_2H_4 is 2 eV, indicating a dominant contribution of HOMO to the ionization of C_2H_4. Actually, according to our calculation, the transition amplitude of HOMO-1 is at least two orders

TABLE II. The ionization potentials and symmetries of the molecular orbitals.

I_p (eV)	C_2H_4	C_2H_6
HOMO	$10.5b_{3u}$	$11.5e_g$
HOMO-1	$12.5b_{3g}$	$12.1a_{1g}$
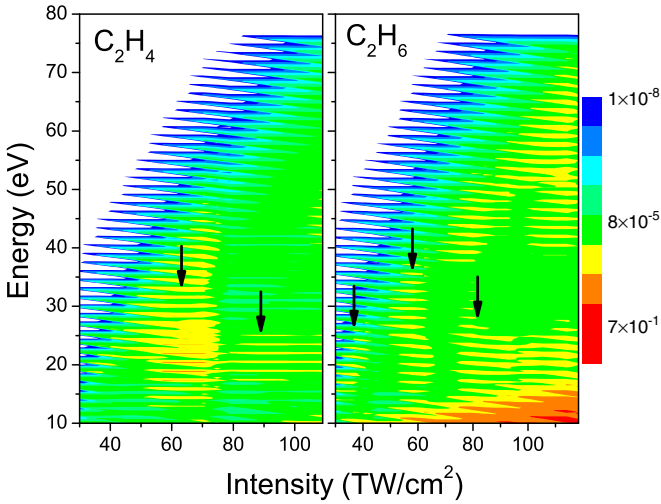
FIG. 3. The simulated ATI spectra of C_2H_4 and C_2H_6.

of magnitude smaller than that of HOMO for C_2H_4. For C_2H_6, on the other hand, the difference is only 0.6 eV, and the contributions become comparable between HOMO-1 and HOMO.

The simulated spectra of C_2H_4 and C_2H_6 are shown in Figs. 3 and 4. Generally, the calculation reproduces most of the features in the measurement in Figs. 1 and 2: two RLEs regions appear at around 60 and 85 TW/cm^2, respectively, in C_2H_4, whereas at least three RLE areas appear at around 35, 60, and 85 TW/cm^2, respectively, in C_2H_6. As shown in Fig. 3, the strong and weak RLEs also emerge alternatively but with different orders for the two molecules. For C_2H_4 the first RLE is very strong and the second is weak, while for C_2H_6 the second RLE is strong and the other two are weak (see Fig. 4).

Clearly, the different RLE structures of the two molecules can be attributed to their different orbital structures. For C_2H_4, due to the dominant contribution of the HOMO of which the wave function contains only C π contributions, it is very clear
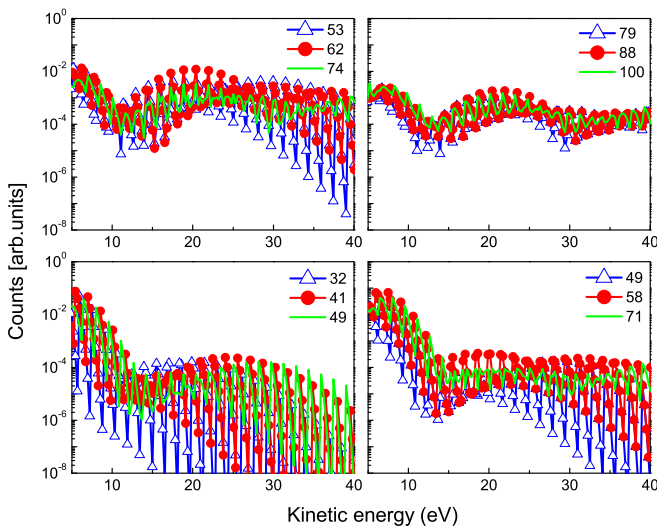
FIG. 4. The simulated electron kinetic energy spectra of C_2H_4 [panels (a) and (b)] and C_2H_6 [panels (c) and (d)].
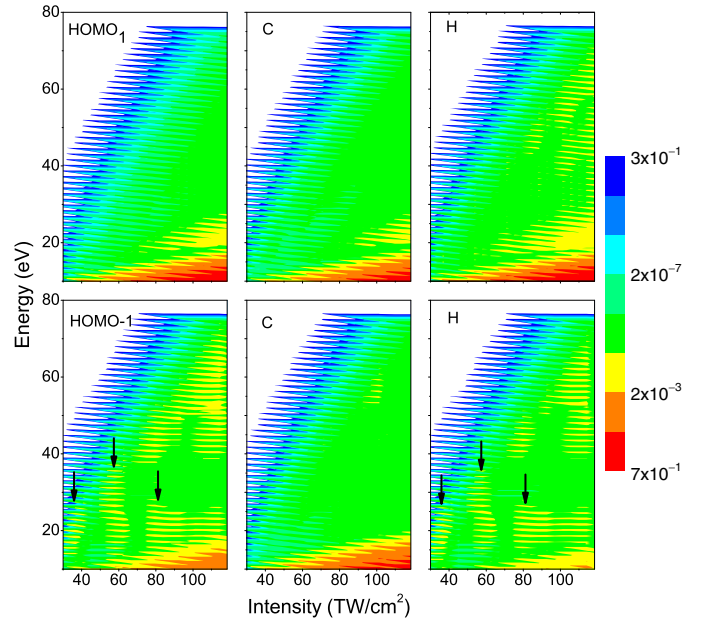
FIG. 5. The simulated ATI spectra corresponding to different occupied orbitals of C_2H_6: HOMO$_1$ in the first row and HOMO-1 in the second row. The spectra corresponding to C and H components in each orbital are also shown in the second and third columns, respectively.

that the RLE structure of C_2H_4 comes from C centers in the HOMO. For C_2H_6, the situation is much more complex. Both HOMOs and HOMO-1 contribute significantly and both C and H atomic functions are included in the wave function of all orbitals. Owing to the LCAO approximation, we can separate the contribution of different components of the wave function. In Fig. 5 we show the individual ATI spectra of HOMO and HOMO-1 of C_2H_6, and also the spectra corresponding to different components which are obtained by performing calculations with only C or H atomic orbitals included. It is noted that, although here we only show the spectra for one of the degenerate HOMOs, the spectra of the other one are similar. As can be seen in Fig. 5, the RLE structure of C_2H_6 comes only from H components of HOMO-1, while C in all orbitals and H in HOMO show no RLE structure.

The appearance or absence of the RLE structure for different orbitals and cores is ascribed to the wave functions. In the view of "quantum orbits," the RLE structures originate from constructive interference of large number of multiple-return orbits. Compared to atoms, the HATI transition amplitude $M_{\mathbf{p}}^{\mathrm{resc}}$ [Eq. (7)] of molecule contains the additional interference factor $\cos(\mathbf{k} \cdot \mathbf{R}_0/2)$ or $\sin(\mathbf{k} \cdot \mathbf{R}_0/2)$ *depending on orbital symmetry* [28]. Generally, electrons in multiple-return trajectories return to the core near extrema of the electric field, the intermediate momentum $\mathbf{k}$ is close to zero. So for the orbital with $\gamma = -1$ in Eq. (4), the above interference factor $\sin(\mathbf{k} \cdot \mathbf{R}_0/2)$ is close to zero and there will be a suppressing effect on the RLE structure. While for the orbital with $\gamma = -1$, the interference factor $\cos(\mathbf{k} \cdot \mathbf{R}_0/2)$ is approximately equal to one and the RLE structure will survive [24]. The results in Figs. 3 and 5 can be understood based on the above mechanism. For the HOMO of C_2H_4 which is dominant, the sign in Eq. (4)

for the p functions on the two C centers is "+," as shown in Table I, so the RLE structure is apparently visible. But for C_2H_6, the signs of the linear combinations of the p orbitals on the C centers in both the HOMO and HOMO-1 orbitals are "−," while the corresponding signs in all H components are "+." So the RLE structure is absent in the spectra of C cores but should be visible for H cores in all orbitals of C_2H_6. However, spectrum of the H components in $HOMO_1$, as well as in $HOMO_2$ (not shown here), of C_2H_6 shows no RLE structure. This can be attributed to the fact that these two orbitals have e_g symmetry so that, as shown in Table I, the signs in front of the pairs of H are opposite, hence their corresponding terms in the HATI transition amplitude $M_{\mathbf{p}}^{\text{resc}}$ [Eq. (3)] will cancel each other out. It is noted that this occurs exactly only when the values of interference factor corresponding to the H pairs are the same, which is only satisfied when the intermediate momentum $\mathbf{k} = 0$. For nonzero $\mathbf{k}$, the factors usually are not the same since the coordinates $\mathbf{R}_0$ for the two pairs of H are different; however, they still cancel each other largely since, as mentioned before, the intermediate momentum is close to zero. The situation of $HOMO_2$ is similar but, for HOMO-1, the RLE structure survives since the signs of the three pairs of H are all the same.

According to Ref. [29], for atoms there are two different types of RLEs with different intensity dependence. The intensity dependence of the first type is comparatively smooth while that of the second type is extremely sharp. Moreover, the two types of RLEs appear alternatively, which depends on the angular momentum of the initial state. For s states ($l = 0$), the sharp RLE appears at an intensity corresponding to channel closing of even absorbed photon number while for p states ($l = 1$), it occurs at channel closing of odd absorbed photon number. The above theory for atoms is also applicable for molecules considered here since the molecules' orbitals are constructed based on atomic orbitals. If we only pay attention to the orbitals contributing to the RLEs, it is clear that the p state is dominant in the wave function of the C cores in the b_{3u} HOMO of C_2H_4 while there is only s state components included in the wave function of the H cores in the a_{1g} HOMO-1 of C_2H_6. Although for both of C_2H_4 and C_2H_6, the photon number for channel closing of the first (second) RLEs is $n = 9$ ($n = 10$), they belong to different types of RLEs due to different parity of the atomic orbitals included in the ground state. This explain why the two molecules show different sequences of strong and weak RLEs.

In conclusion, we study the resonance-like enhancement effect in strong-field ionization of polyatomic molecular. We found that, for C_2H_4, C–C cores in the HOMO orbital are responsible for the RLE structures, while for C_2H_6, they do not contribute to RLE due to destructive interference but the hydrogen cores of the bonding HOMO-1 orbital give rise to the multiple RLEs. Moreover, our work provides clear experimental evidence of the existence of two types of the RLE and their dependence on the parity of the ground state. Our results, which can be considered as strong support for the channel-closing mechanism of the RLE, reveals the important role of low-lying orbitals in the RLE and different nuclei play different roles in the HATI of molecules. This work sheds important new light onto laser-assisted ultrafast imaging of molecules.

[1] C. I. Blaga, J. Xu, A. D. DiChiara, E. Sistrunk, K. Zhang, P. Agostini, T. A. Miller, L. F. DiMauro, and C. D. Lin, Nature (London) **483**, 194 (2012).

[2] P. Salières, A. Maquet, S. Haessler, J. Caillat, and R. Taïeb, Rep. Prog. Phys. **75**, 062401 (2012).

[3] M. Meckel, D. Comtois, D. Zeidler, A. Staudte, D. Pavičić, H. C. Bandulet, H. Pépin, J. C. Kieffer, R. Dörner, D. M. Villeneuve, and P. B. Corkum, Science **320**, 1478 (2008).

[4] J. Itatani, J. Levesque, D. Zeidler, H. Niikura, H. Pépin, J. C. Kieffer, P. B. Corkum, and D. M. Villeneuve, Nature (London) **432**, 867 (2004).

[5] C. Vozzi, M. Negro, F. Calegari, G. Sansone, M. Nisoli, S. De Silvestri, and S. Stagira, Nat. Phys. **7**, 822 (2011).

[6] B. K. McFarland, J. P. Farrell, P. H. Bucksbaum, and M. Gühr, Science **322**, 1232 (2008).

[7] O. Smirnova, Y. Mairesse, S. Patchkovskii, N. Dudovich, D. Villeneuve, P. Corkum, and M. Y. Ivanov, Nature (London) **460**, 972 (2009).

[8] P. B. Corkum, Phys. Rev. Lett. **71**, 1994 (1993).

[9] K. J. Schafer, B. Yang, L. F. DiMauro, and K. C. Kulander, Phys. Rev. Lett. **70**, 1599 (1993).

[10] M. Okunishi, R. Itaya, K. Shimada, G. Prümper, K. Ueda, M. Busuladžić, A. Gazibegović-Busuladžić, D. B. Milošević, and W. Becker, Phys. Rev. Lett. **103**, 043001 (2009).

[11] H. Kang, W. Quan, Y. Wang, Z. Lin, M. Wu, H. Liu, X. Liu, B. B. Wang, H. J. Liu, Y. Q. Gu, X. Y. Jia, J. Liu, J. Chen, and Y. Cheng, Phys. Rev. Lett. **104**, 203001 (2010).

[12] M. Okunishi, H. Niikura, R. R. Lucchese, T. Morishita, and K. Ueda, Phys. Rev. Lett. **106**, 063001 (2011).

[13] C. Altucci, R. Velotta, E. Heesel, E. Springate, J. P. Marangos, C. Vozzi, E. Benedetti, F. Calegari, G. Sansone, S. Stagira, M. Nisoli, and V. Tosa, Phys. Rev. A **73**, 043411 (2006).

[14] M. P. Hertlein, P. H. Bucksbaum, and H. G. Muller, J. Phys. B: At., Mol. Opt. Phys. **30**, L197 (1997).

[15] P. Hansch, M. A. Walker, and L. D. Van Woerkom, Phys. Rev. A **55**, R2535 (1997).

[16] F. Grasbon, G. G. Paulus, H. Walther, P. Villoresi, G. Sansone, S. Stagira, M. Nisoli, and S. De Silvestri, Phys. Rev. Lett. **91**, 173003 (2003).

[17] H. G. Muller and F. C. Kooiman, Phys. Rev. Lett. **81**, 1207 (1998).

[18] H. G. Muller, Phys. Rev. Lett. **83**, 3158 (1999).

[19] J. Wassaf, V. Véniard, R. Taïeb, and A. Maquet, Phys. Rev. Lett. **90**, 013003 (2003).

[20] R. Kopold and W. Becker, J. Phys. B: At., Mol. Opt. Phys. **32**, L419 (1999).

[21] S. V. Popruzhenko, Ph. A. Korneev, S. P. Goreslavski, and W. Becker, Phys. Rev. Lett. **89**, 023001 (2002).

[22] G. G. Paulus, F. Grasbon, H. Walther, R. Kopold, and W. Becker, Phys. Rev. A **64**, 021401(R) (2001).

[23] C. Wang, Y. Tian, S. Luo, W. G. Roeterdink, Y. Yang, D. Ding, M. Okunishi, G. Prümper, K. Shimada, K. Ueda, and R. Zhu, Phys. Rev. A **90**, 023405 (2014).

[24] W. Quan, X. Y. Lai, Y. J. Chen, C. L. Wang, Z. L. Hu, X. J. Liu, X. L. Hao, J. Chen, E. Hasović, M. Busuladžić, W. Becker, and D. B. Milošvić, Phys. Rev. A **88**, 021401(R) (2013).

[25] G. G. Paulus, W. Becker, W. Nicklich, and H. Walther, J. Phys. B: At., Mol. Opt. Phys. **27**, L703 (1994).

[26] M. Okunishi, K. Shiamada, G. Prümper, D. Mathur, and K. Ueda, J. Chem. Phys. **127**, 064310 (2007).

[27] C. Wang, M. Okunishi, R. R. Lucchese, T. Morishita, O. I. Tolstikhin, L. B. Madsen, K. Shimada, D. Ding, and K. Ueda, J. Phys. B: At., Mol. Opt. Phys. **45**, 131001 (2012).

[28] D. B. Milošević, Phys. Rev. A **74**, 063404 (2006); M. Busuladžić, A. Gazibegović-Busuladžić, D. B. Milošević, and W. Becker, Phys. Rev. Lett. **100**, 203003 (2008); Phys. Rev. A **78**, 033412 (2008); E. Hasović and D. B. Milošević, *ibid.* **89**, 053401 (2014).

[29] D. B. Milošević, E. Hasović, M. Busuladžić, A. Gazibegović-Busuladžić, and W. Becker, Phys. Rev. A **76**, 053410 (2007).